Meniscus of a ferrofluid around a vertical cylindrical wire carrying electric current

Thomas John, Kathrin May, and Ralf Stannarius
Institut für Experimentelle Physik, Fakultät für Naturwissenschaften, Universität Magdeburg, Universitätsplatz 2, D-39106 Magdeburg, Germany
(Received 4 February 2011; published 9 May 2011)

We study the meniscus profiles of ferrofluids in the magnetic field of a vertical current-carrying wire. Measurements of the free ferrofluid surface profile are quantitatively compared with numerical calculations. The theoretical model leads to a second-order ordinary differential equation. All material parameters are determined in independent experiments, therefore no fitting parameters are involved in the calculations. The experimental results can be modeled by the equilibrium of magnetic, gravitational, and interface tension forces. The classical model that neglects interface tension yields significant deviations from the experimental profiles in the parameter range studied.

DOI: 10.1103/PhysRevE.83.056308 PACS number(s): 47.65.−d, 47.85.−g

I. INTRODUCTION

Ferrofluids are stable suspensions of nanometer-sized magnetic monodomain particles in a carrier fluid (see, e.g., Refs. [1–3]). The particles are coated with a surfactant to inhibit agglomeration. The suspensions are stable because of Brownian motion. This is in contrast to magnetorheological fluids where the particle diameters are on the micrometer scale. However, both types of magnetic fluids combine the common hydrodynamic properties of fluids with the opportunity to interact with magnetic fields. This combination gives rise to a lot of interesting applications [4] (e.g., liquid seals around the rotating shafts in hard disks, cooling of voice coils in loudspeakers, or contrast agents for magnetic resonance imaging in medicine). For hydrodynamics it is interesting because an additional volume force can be easily applied using a magnetic field. A popular effect for demonstrations is the Rosensweig or normal field instability, where a flat magnetic fluid surface becomes unstable in an external magnetic field [3,5–8]. In the case of many other geometries (e.g., capillary tubes, sandwich cells), the surface tension plays an important role [9–13]. Experiments and calculations regarding the geometry of a meniscus of ferrofluid at a flat wall in a homogeneous magnetic field can be found in Refs. [14,15]. Recently, a solitary wave propagation on a ferrofluid surface around a current-carrying horizontal wire was realized experimentally [16,17].

Here we investigate quantitatively the static meniscus profile of a ferrofluid surface around a current-carrying vertical wire, first observed in 1964 by Neuringer and Rosensweig [18]. In contrast to earlier descriptions of the meniscus profile [1,18,19], the surface tension is taken into account in our model. The rotational symmetry of the experiment simplifies the theoretical description of a free-surface boundary value problem to an ordinary second-order nonlinear differential equation, which is solved numerically [20]. In contrast to the experimental work of Bacri *et al.* [21–23] with a microscopic wire diameter of 50 μm, we use a wire with a diameter of 1.9 mm and therefore higher currents up to 100 A. Because the diameter of the wire is of the same order of magnitude as the capillarity length $K^{-1} = \sqrt{\sigma/(\varrho g)} \simeq 1.7$ mm, with surface tension σ, density ϱ of the ferrofluid, and gravitational acceleration g, the analytical solutions for various physical limits (see, e.g., Ref. [21]) are not suitable in our experiment. All involved material parameters are known, therefore no fitting parameters are used in the comparison of measurements with numerical predictions.

II. EXPERIMENTAL SETUP AND MATERIAL PARAMETERS

To provide the azimuthal magnetic field $H(r) = I/(2\pi r)$ in a distance r from the wire axis we use a current-carrying vertical-straight cylinder wire made from copper with a thin lacquer isolation, diameter $2R = 1.9$ mm. The current I is generated with a welding transformer (Lorch, Handy-Tig 210) and measured with a shunt and a direct-current (dc) voltmeter (Keithley, Multimeter 2010). A maximum dc current of 100 A can be achieved. Due to the adaptive regulation inside the transformer, the current varies around the average dc amplitude with in the frequency range of 100 kHz. This has been measured with an oscilloscope (Meilhaus, MEphisto Scope). The profiles of the ferrofluid in the experiments are only sensitive to the time-averaged current, thus the high-frequency oscillations are irrelevant. This has been verified for exemplary currents by comparing the results with those obtained with a 12 V car battery as power supply. A cylindrical glass vessel around the wire, diameter 30 mm, height 15 mm, contains the ferrofluid. To avoid the influences of the vessel during image recording, the vessel is filled up to a level slightly above the outer border of the vessel, held by the surface tension of the ferrofluid. When a meniscus around the wire forms, the rising ferrofluid leads only to a very small depression of the planar level in the dish.

The setup is homogeneously illuminated from the back and images are taken with a USB microscope (dtn, digicam2.0) with a resolution of 1600×1200 pixel, see Fig. 1. An alternative method using the reflex of a laser beam is described in Refs. [14,15].

To avoid thermal heating of the wire and the surrounding ferrofluid we apply strong currents only for a few seconds. After the desired current has been switched on, the meniscus profile becomes stationary in approximately 1 s, an image is recorded, and the transformer is switched off again. To get a perception of the sample temperatures, we have measured the temperature of the wire and the surface of the ferrofluid with a thermal imaging camera, see Fig. 2. At a current of 70 A,

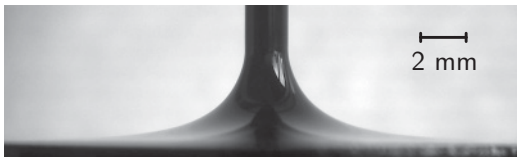

FIG. 1. Picture of the meniscus of EMG 909 around the current-carrying wire at 70 A ($H_{max} = 12$ kA/m at the wire surface).

the wire is heated up from room temperature to 75° C after 5 s. The temperature of the ferrofluid around the wire is still below 30° C at the image recording time. Only a very thin layer of the ferrofluid is heated up. A few minutes later the next profile is taken. All measurements where performed with the bulk ferrofluid at room temperature.

The ferrofluids APG S21 and EMG 909 are commercially available from Ferrotec [24]. The densities ϱ are 1140 kg m^{-3} for APG S21 and 1020 kg m^{-3} for EMG 909 [25], respectively. To obtain the interface tension σ respective to air we use the capillary rise method with a capillary diameter of 1.08 mm: $\sigma_{APGS21} = 0.0331$ N m^{-1} and $\sigma_{EMG909} = 0.0258$ N m^{-1} with an accuracy of 3%.

In some experiments, we study the depression of the interface of a ferrofluid stacked above a heavier, immiscible liquid. To cover the nonmagnetic fluid with the ferrofluid, we use a glycerol/water mixture with the volume ratio 1 : 1. It has a density of 1148 kg m^{-3} comparable to the ferrofluid EMG 909. The interface tension of $\sigma_{EMG909/GlyH2O} = 0.014$ N m^{-1} has been measured with the pendant drop method with a tube diameter of 1.08 mm. The magnetizations of both ferrofluids have been measured with a vibrating sample magnetometer (LakeShore, Model 7407), see Fig. 3. The initial susceptibility is extracted from the datasets, $\chi_i = 0.65$ for APG S21 and $\chi_i = 0.61$ for EMG 909. Because the experiments can change the magnetic properties of the ferrofluids, we measured the magnetization of the samples four months later again. The magnetizations of the samples decreased by 6%. This change does not influence the calculated profiles below significantly.

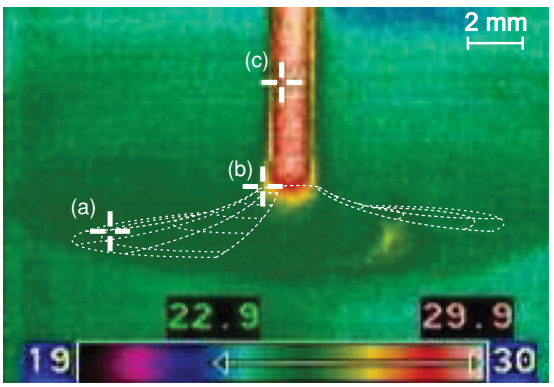

FIG. 2. (Color online) Thermal imaging camera picture of the wire with ferrofluid, taken 2 s after a current onset of 70 A. This camera view is inclined with an angle of 45° from the top. The dashed lines indicate the approximate ferrofluid profile. The determined temperatures at selected points are (a) 25.1° C, (b) 27° C, and (c) 30° C.

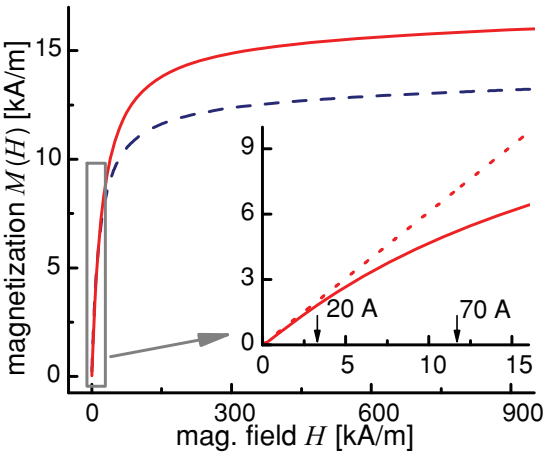

FIG. 3. (Color online) Measured magnetizations $M(H)$ of the ferrofluids EMG 909 (solid red line) and APG S21 (dashed blue line). The inset shows a magnification for EMG 909 only. A dotted line indicates the assumed linear relation $M = \chi_i H$ with $\chi_i = 0.61$. Arrows marks the corresponding amplitude of the maximum magnetic field at the edge of the wire at 20 A and 70 A ($H_{max} = 3.4$ kA/m and $H_{max} = 12$ kA/m).

III. CALCULATION OF MENISCUS PROFILES

We calculate the interface between the ferrofluid and a nonmagnetic fluid under the influence of gravity, surface tension and a magnetic field of the current-carrying vertical cylindrical wire. The rotational symmetry of the problem reduces the computation from a free two-dimensional (2D) interface to a one-dimensional (1D) height profile $\zeta(r)$, where r is the distance to the wire axis and ζ is the height of the meniscus with $\zeta(r \to \infty) = 0$. As mentioned in Ref. [20], the minimization of the total energy can be used to obtain the function $\zeta(r)$ under the inclusion of the interface tension. An alternative method is described in Refs. [21–23]. For small applied fields, the magnetization of the ferrofluid can be linearized to $M(H) = \chi_i H$. A simple derivation with the

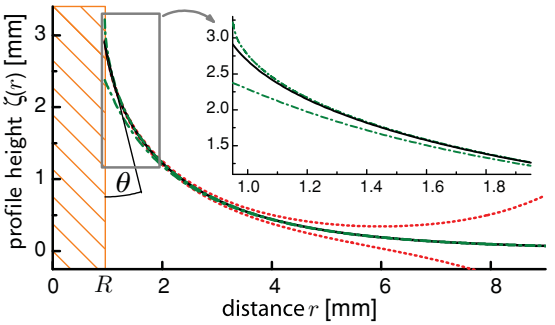

FIG. 4. (Color online) Calculated profiles of the ferrofluid–air interface for APG S21 at a current of 70 A and a contact angle θ of 10° with the correct initial height of 2.9 mm (solid black line) to satisfy the physically relevant boundary condition $\zeta(r \to \infty) = 0$. Solutions of Eq. (1) at 0.5% higher and lower initial heights are shown as dotted gray (red) lines. These solutions do not fulfill the physically relevant boundary condition. A dramatic change of the initial slope between 1° and 30° (dash-dotted green line) leads only to changes of the profiles in the vicinity of the wire surface. The inset shows the magnified region near the wire. The patterned area indicates the wire.

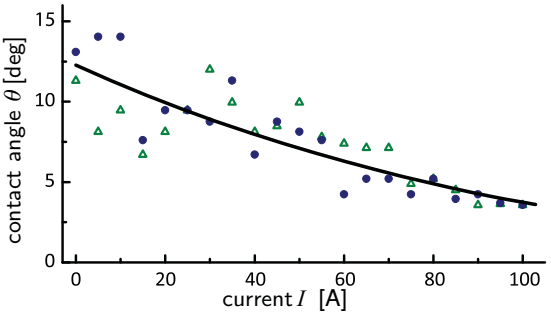

FIG. 5. (Color online) Extracted (APG S21 dots, EMG 909 triangles) contact angles θ between the wire and the fluid surface. The solid line guides the eye.

help of this magnetization and neglecting the interface tension can be found in Ref. [1]: $\zeta_0 \propto r^{-2}$. For large magnetic fields, the magnetization of the ferrofluid saturates and one can find $\zeta_S \propto r^{-1}$ [19]. Taking the surface tension into account, a limit for thin wires and without magnetic fields can be found in Ref. [21]. Here we focus on the numerical solution of the governing equation with a linear magnetization relation because it has been shown in Ref. [20] that the assumption of a Langevin-type magnetization leads only to small corrections of the calculated profiles in the vicinity of the wire, which are relevant only at high applied electric currents. In the limit of a linear magnetization a nonlinear second-order ordinary differential equation determines the height of the profile [20]

$$g|\varrho - \tilde{\varrho}|\zeta - \frac{\mu_0 \chi_i}{8\pi^2}\frac{I^2}{r^2} - \sigma\frac{\zeta' + \zeta'^3 + r\zeta''}{(1+\zeta'^2)^{3/2}}\frac{1}{r} = 0, \qquad (1)$$

with the gravitational acceleration g, and the difference of the densities ϱ for the ferrofluid and $\tilde{\varrho}$ for the nonmagnetic fluid. The primes correspond to spatial derivatives. Neglecting the interface tension σ leads immediately to

$$\zeta_0(r) = \frac{\mu_0 \chi_i}{8\pi^2|\varrho - \tilde{\varrho}|g}\frac{I^2}{r^2}. \qquad (2)$$

The physically relevant solution of Eq. (1) has to satisfy the two boundary conditions $\zeta(r \to \infty) = 0$ and $\zeta'(R) = -\tan(90^\circ - \theta)$, with the angle θ as the slope of the interface at the radius of the wire R, see Fig. 4. The angle θ is extracted from experimentally determined profiles. To solve the boundary value problem (1) numerically, we use an

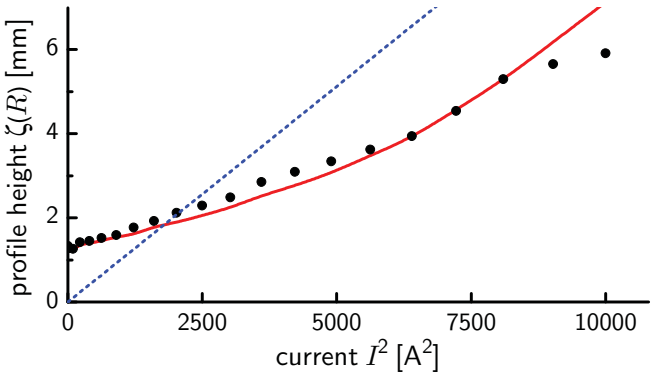

FIG. 7. (Color online) Measured (black dots) and calculated heights (solid red line) of the profiles at $r = 0.95$ mm (contact with the wire) for the ferrofluid APG S21. The dotted blue line represents $\zeta_0(R) \propto I^2$, neglecting the interface tension.

adaptive shooting method. By principle, Eq. (1) is integrated forward with the initial value $\zeta'(R)$ and with a first guess of an initial value $\zeta(R)$. Then $\zeta(R)$ is varied until the first boundary condition is fulfilled (i.e., ζ approaches zero for large distances from the wire). This method converges rapidly because of the smooth response of the solution to small changes in the initial value $\zeta(R)$, see Fig. 4. Even a small change of this height produces incorrect solutions where $\zeta(r \to \infty)$ is not zero (red dotted lines in Fig. 4). In fact, these solutions correspond to situations where the ferrofluid is bound at an outer cylindrical container wall with some nonzero contact angle. On the other hand, the influence of the initial slope of ζ is small, see Fig. 4. This justifies the usage of the experimentally determined $\zeta'(R)$ in the calculations irrespective of the experimental uncertainties of this value.

In Refs. [21,26], analytical equations are given that yield the profiles also in the absence of a magnetic field, in the limit of a capillarity length $K^{-1} = \sqrt{\sigma/(\varrho g)}$, much larger than the wire radius R. This limit is not fulfilled in our experiments where $K^{-1} \approx 1.7$ mm.

IV. FERROFLUID–AIR INTERFACE

In systems with a ferrofluid–air interface one can substitute the expression $|\varrho - \tilde{\varrho}|$ in Eq. (1) by ϱ. The experimental problem in the determination of the meniscus profile is the

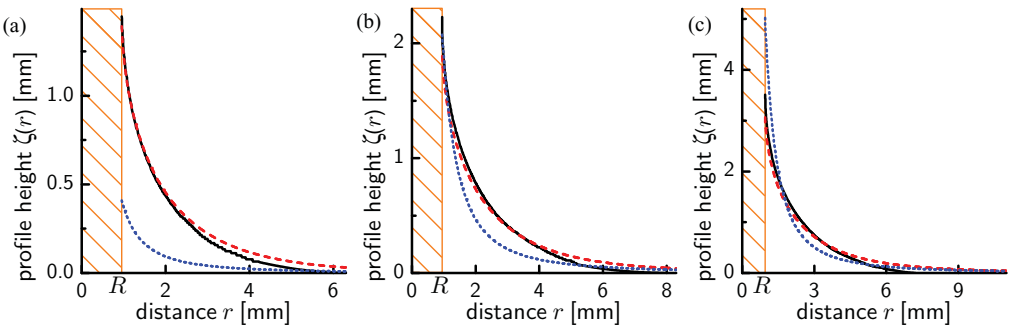

FIG. 6. (Color online) Profiles of the ferrofluid–air interface: measured (solid black line), calculated with (dashed red line) and without (dotted blue line) interface tension for APG S21 at a carrying-current wire of (a) 20 A, (b) 45 A, and (c) 70 A. The patterned area indicates the width of the wire.

boundary condition of the surface profile at the wire, which depends upon the wetting of the wire by the ferrofluid. We have not determined the equilibrium contact angle of the ferrofluid at the bare wire since that angle is irrelevant for the experiment. After the first experiment with a fresh wire, when a meniscus has been created, the wire remains coated with a thin layer of ferrofluid that creeps down only very slowly. Therefore it is useful to perform quantitative measurements with wires that are already wetted by the ferrofluid.

If we increase the electric current of a nonwetted wire slowly and continuously, the profile height at the wire surface does not ascend in the same continuous manner. It rises in an irregular stick-slip motion at the wire surface (see, e.g., Refs. [27,28]). To obtain reproducible profiles, we usually wet the wire with ferrofluid before the first quantitative measurement: We apply a short current burst to prepare a very thin film of ferrofluid on the surface of the wire. The thickness of the film is below the experimental resolution, but it is visible by a change (darkening) of the color of the wire surface. This thin film persists for a couple of minutes. At this film, a macroscopic contact angle is still observable. Theoretical models to explain such microscopic and macroscopic wetting behavior are based on generalized capillary pressures (see, e.g., Ref. [29] and references therein). An earlier publication dealing with ferrofluid around a cylindrical wire is Ref. [23]. To compare experimental profiles with numerical calculations, the approximate value of the contact angle is necessary. We determine the contact angle θ from the extracted profiles $\zeta(r \to R)$ shown in Fig. 5. For both ferrofluids, the contact angle is about 10° and it decreases at higher magnetic fields, respectively, stronger currents. However, for the numerical calculation of the profiles, as well as for the experimental realization, this parameter plays a role only in the vicinity of the wire, see above.

In Fig. 6, measured and calculated profile heights are depicted. At zero and small applied currents, the surface of the ferrofluid is almost completely dominated by the interface tension. With increasing currents, the magnetic energy becomes dominant and the calculated profiles are less sensitive to the interface tension. At all currents, the inclusion of the interface tension in the calculations leads to a smaller curvature in the profiles. An obvious characteristic of the profiles is the height $\zeta_0 = \zeta(R)$ at the contact with the wire. Neglecting the interface tension gives a $\zeta_0 \propto I^2$ relation. Measured and calculated profile heights $\zeta(R)$ are depicted in Fig. 7 as a function of I^2. In the limit of vanishing currents, the height is given by the interface tension alone.

V. FERROFLUID–LIQUID INTERFACE

For applications, often the interface between ferrofluid and an immiscible nonmagnetic liquid is interesting. In demonstrations it is useful to overcover or undercover the ferrofluid with an immiscible liquid with similar density to reduce the influence of the gravity and thereby to obtain much higher profiles. In this case, the density difference between the fluids is relevant in the term of the gravitational energy in Eq. (1). We cover a mixture of glycerol/water in a volume ratio of 1:1 with the ferrofluid EMG 909. To avoid optical distortions we use a rectangular cuboid container made from transparent plastic instead of a cylindrical glass container. The profile of the ferrofluid grows downward in the glycerol/water mixture when a current applied. A photo of the deformed ferrofluid surface is shown in Fig. 8 together with measured and calculated profiles. As expected, the amplitudes of the surface deformations are much bigger. As in the ferrofluid–air interface, the difference between the measurements and the calculated profiles without interface tension [see Eq. (2)] at intermediate currents can be explained taking the interface tension into account.

VI. SUMMARY

We presented a quantitative comparison of experimental meniscus profiles of a ferrofluid around a current-carrying wire with calculated profiles. The interface tension was taken into account. The rotational symmetry of the experiment reduces the free surface problem to a comparably simple nonlinear second-order ordinary differential equation. The boundary conditions are a flat surface at large distances from the wire and a contact angle at the wire. Calculations prove that the contributions of the contact angle to the profile are localized to the vicinity of the current-carrying wire. The contact angle, determined from extracted profiles, shows a slight dependence on the current. We would like to mention that the contact angle problem has been disregarded in earlier studies of ferrofluid menisci completely. In our experiment

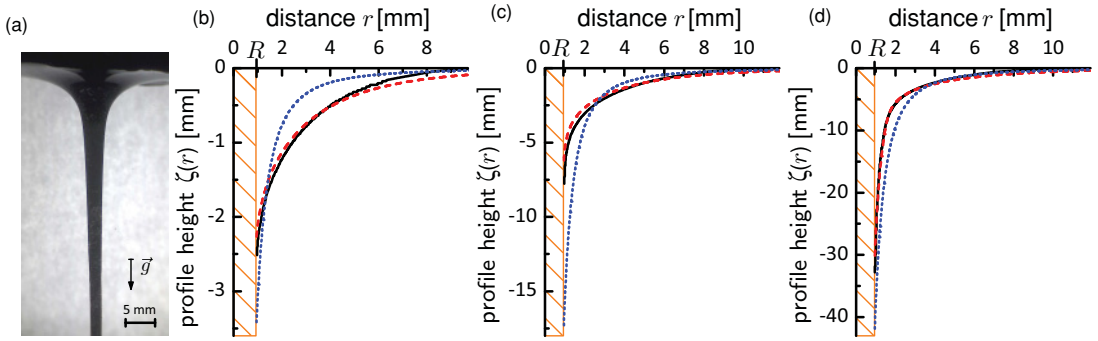

FIG. 8. (Color online) (a) Picture of the ferrofluid EMG 909–glycerol/water interface at 70 A. (b–d) Profiles extracted from photos and calculated profiles of the interface at currents of (b) 20 A ($H_{max} = 3.4$ kA/m), (c) 45 A ($H_{max} = 7.5$ kA/m), and (d) 70 A ($H_{max} = 12$ kA/m). Line styles are the same as in Fig. 6.

we resolve the profile in the immediate vicinity of the wire sufficiently well so that the influence of the contact angle is noticeable. A detailed investigation can be the topic of further studies. The experimental geometry with circular magnetic field lines and a surface with the same geometry prevent the refraction of the magnetic field. The field lines are parallel to the local ferrofluid surface everywhere. The nonlinear magnetization $M(H)$ of the ferrofluids can be neglected in the description of our experiment because the magnitude of the magnetic field is moderate and decays rapidly with increasing distance from the wire in our geometry. In the limit of a vanishing magnetic field, the interface tension alone governs the surface deformations (capillary rise or depression). At intermediate magnetic fields (currents of $\approx$50 A in a wire with diameter of $\approx$2 mm, i.e., maximum field strengths of the order of 10 kA/m) the deviations between measured menisci and profiles calculated without the inclusion of the interface tension amount to up to 50% of the profile heights. At higher magnetic fields, the difference becomes smaller since the ratio of interface energy to magnetic field energy decreases with I^{-2}. The numerical approach applied here includes the different analytical approximations for vanishing surface tensions and vanishing gravitational forces that have been presented in the earlier literature [21,23,26].

ACKNOWLEDGMENTS

The authors acknowledge Adrian Lange for stimulating discussions and Harald Engler for magnetization measurements in the group of Stefan Odenbach at the Technische Universität Dresden. We also have to thank Wolfgang Fischer from the Institut für Elektrische Energiesysteme at the Universität Magdeburg for the supply of transformers and power resistors.

[1] R. E. Rosensweig, *Ferrohydrodynamics* (Cambridge University Press, Cambridge, England, 1985).
[2] E. Blums, A. Cebers, and M. M. Maiorov, *Magnetic Fluids* (Walter de Gruynter, Berlin, 1997).
[3] *Colloidal Magnetic Fluids*, Lecture Notes in Physics, Vol. 763, edited by S. Odenbach (Springer, New York, 2009).
[4] B. M. Berkovsky and V. Bashtovoy, *Magnetic Fluids and Applications Handbook* (Begell House Publishers, New York, 1996).
[5] M. D. Cowley and R. E. Rosensweig, J. Fluid Mech. **30**, 671 (1967).
[6] J.-C. Bacri and D. Salin, J. Physique Lett. **45**, 559 (1984).
[7] A. Lange, B. Reimann, and R. Richter, Phys. Rev. E **61**, 5528 (2000).
[8] C. Gollwitzer, M. Krekhova, G. Lattermann, I. Rehberg, and R. Richter, Soft Matter **5**, 2093 (2009).
[9] C. Flament, S. Lacis, J.-C. Bacri, A. Cebers, S. Neveu, and R. Perzynski, Phys. Rev. E **53**, 4801 (1996).
[10] V. Bashtovoi, P. Kuzhir, and A. Reks, J. Magn. Magn. Mater. **252**, 265 (2002).
[11] V. Bashtovoi, G. Bossis, P. Kuzhir, and A. Reks, J. Magn. Magn. Mater. **289**, 376 (2005).
[12] V. Polevikov and L. Tobiska, J. Magn. Magn. Mater. **289**, 379 (2005).
[13] S. Elborai, D.-K. Kim, X. He, S.-H. Lee, S. Rhodes, and M. Zahn, J. Appl. Phys. **97**, 10Q303 (2005).
[14] R. Rosensweig, S. Elborai, S.-H. Lee, and M. Zahn, J. Magn. Magn. Mater. **289**, 192 (2005).
[15] S. M. Elborai, Ph.D. thesis, Massachusetts Institute of Technology, 2006.
[16] D. Rannacher and A. Engel, New J. Phys. **8**, 108 (2006).
[17] E. Bourdin, J.-C. Bacri, and E. Falcon, Phys. Rev. Lett. **104**, 094502 (2010).
[18] J. I. Neuringer and R. E. Rosensweig, Phys. Fluids **7**, 1927 (1964).
[19] D. A. Krueger and T. B. Jones, Phys. Fluids **17**, 1831 (1974).
[20] T. John, D. Rannacher, and A. Engel, J. Magn. Magn. Mater. **309**, 31 (2007).
[21] J.-C. Bacri, R. Perzynski, D. Salin, and F. Tourinho, Europhys. Lett. **5**, 547 (1988).
[22] J.-C. Bacri, C. Frenois, R. Perzynski, and D. Salin, Rev. Phys. Appl. **23**, 1017 (1988).
[23] J. C. Bacri, R. Perzynski, and D. Salin, Lecture Notes Phys. **354**, 1 (1990).
[24] We used commercial ferrofluis APG S21 and EMG 909 from Ferrotec GmbH Germany, for material parameters see also [www.ferrotec-europe.de.]
[25] There is a typesetting error in Ref. [20], the measured density for EMG 909 is 1020 m^{-3}.
[26] Y. Murakami, T. Ohkita, and K. Gotoh, J. Phys. Soc. Jpn. **61**, 1964 (1992).
[27] M. E. R. Shanahan, Langmuir **11**, 1041 (1995).
[28] F. Wu-Bavouzeta, J. Clain-Burckbuchlera, A. Buguina, P. G. D. Gennes, and F. Brochard-Wyarta, The Journal of Adhesion **83**, 761 (2007).
[29] J. H. Snoeijer and B. Andreotti, Phys. Fluids **20**, 057101 (2008).